SPANDIDOS PUBLICATIONS

MOLECULAR MEDICINE REPORTS 27: 90, 2023

Knockdown of the long non-coding RNA MALAT1 ameliorates TNF-α-mediated endothelial cell pyroptosis via the miR-30c-5p/Cx43 axis

ZHANG-JIAN YANG[1*], RONG LIU[1*], XIAO-JIAN HAN[2,3], CHENG-LIN QIU[1], GUAN-LIN DONG[1], ZI-QIN LIU[1], LI-HUA LIU[1], YAN LUO[1] and LI-PING JIANG[1]

[1]Jiangxi Provincial Key Laboratory of Drug Targets and Drug Screening, School of Pharmaceutical Science, Nanchang University; [2]Institute of Geriatrics; [3]Department of Neurology, Jiangxi Provincial People's Hospital, First Affiliated Hospital of Nanchang Medical College, Nanchang, Jiangxi 330006, P.R. China

Received November 5, 2022; Accepted February 15, 2023

DOI: 10.3892/mmr.2023.12977

Abstract. Long noncoding RNAs (lncRNAs) are related to the development of atherosclerosis (AS). However, the role of lncRNA metastasis associated lung adenocarcinoma transcript 1 (MALAT1) in tumor necrosis factor-α (TNF-α)-induced rat aortic endothelial cell (RAOEC) pyroptosis, as well as the underlying mechanisms, remain unclear. RAOEC morphology was assessed using an inverted microscope. The mRNA and/or protein expression levels of MALAT1, microRNA(miR)-30c-5p and connexin 43 (Cx43) were assessed using reverse transcription-quantitative PCR (RT-qPCR) and/or western blotting, respectively. The relationships among these molecules were validated by dual-luciferase reporter assays. Biological functions, such as LDH release, pyroptosis-associated protein levels and the proportion of PI-positive cells, were evaluated using a LDH assay kit, western blotting and Hoechst 33342/PI staining, respectively. The present study demonstrated that compared with the control group, the mRNA expression levels of MALAT1 and protein expression levels of Cx43 were significantly up-regulated, whereas miR-30c-5p mRNA expressions levels were significantly decreased in TNF-α-treated RAOEC pyroptosis. Knockdown of MALAT1 or Cx43 significantly attenuated the increase in LDH release, pyroptosis-associated protein expression and PI-positive cell numbers among RAOEC treated using TNF-α, whereas an miR-30c-5p mimic exerted the opposite effect. Furthermore, miR-30c-5p was demonstrated to be a negative regulator of MALAT1 and could also target Cx43. Finally, co-transfection with siMALAT1 and miR-30c-5p inhibitor could attenuate the protective effect of MALAT1 knockdown against TNF-α-mediated RAOEC pyroptosis by upregulation of Cx43 expression. In conclusion, MALAT1 might serve an important role in TNF-α-mediated RAOEC pyroptosis by regulating the miR-30c-5p/Cx43 axis, which would provide a potential novel diagnostic and therapeutic target for AS.

Correspondence to: Professor Li-Ping Jiang, Jiangxi Provincial Key Laboratory of Drug Targets and Drug Screening, School of Pharmaceutical Science, Nanchang University, 461 Bayi Avenue, Nanchang, Jiangxi 330006, P.R. China
E-mail: lpjiang@ncu.edu.cn

[*]Contributed equally

Abbreviations: LncRNAs, long non-coding RNAs; AS, atherosclerosis; MALAT1, metastasis associated lung adenocarcinoma transcript 1; TNF-α, tumor necrosis factor-α; RAOEC, rat aorta endothelial cell; miR, microRNA; Cx43, connexin 43; RT-qPCR, reverse transcription-quantitative PCR; GSDMD, gasdermin D; ASC, apoptosis-associated speck-like protein containing a CARD; GSDMD-N, N-terminus of gasdermin D; HDAC11, histone deacetylase 11; HFD, high-fat diet; HUVECs, human umbilical vein endothelial cells; NLRP3, NLR family pyrin domain containing 3; miRNAs: micro RNAs; FOXO3, forkhead box O3; siRNA, short interfering RNA; GJA1, gap junction protein alpha 1; PI, propidium iodide; NC, negative control; ceRNAs, competitive endogenous RNAs; LDH, lactate dehydrogenase; WT, wild-type; MUT, mutant; Cont, control; C-caspase-1, cleaved caspase-1; F, forward; R, reverse

Key words: atherosclerosis, Cx43, lncRNA MALAT1, miR-30c-5p, pyroptosis

Introduction

Atherosclerosis (AS) is a multifactorial chronic inflammatory disease with high morbidity and mortality rates worldwide (1). Cell death and inflammation are closely related to the pathogenesis mechanisms underlying AS (2,3). The former mainly occurs via apoptosis and necrosis, but a novel type of programmed cell death, that is, pyroptosis, was recently reported (4-6). The classical pyroptosis pathway depends on the activation of caspase-1. Cleaved caspase-1 is a cysteine-dependent protease that serves a vital role in the maturation and secretion of gasdermin D (GSDMD), IL-1β, IL-18 and apoptosis-associated speck-like protein containing a CARD (ASC) (7). In the late stage of pyroptosis, GSDMD is cleaved to generate the N-terminus of GSDMD (GSDMD-N) and

then forms a transmembrane pore for IL-1β and IL-18 release (8). Numerous studies have reported that pyroptosis is related to the inflammatory process of AS (4,5,9). It has been reported that histone deacetylase 11 (HDAC11) promotes AS in high-fat diet (HFD)-fed ApoE-/- mice and that HDAC11 deletion alleviates tumor necrosis factor-α (TNF-α)-induced pyroptosis in human umbilical vein endothelial cells (HUVECs) by suppressing, NLR family pyrin domain containing 3 (NLRP3)/caspase-1/GSDMD and caspase-3/gasdermin E signaling pathways (10). Moreover, hydroxytyrosol acetate inhibits HFD-fed ApoE-/- mice AS by suppressing TNF-α-induced pyroptosis of HUVECs via negative regulation of the HDAC11 related signaling pathway (11). Another study reported that sirtuin 6 reduced TNF-α-induced pyroptosis of vascular endothelial cells by negatively regulating the Lin28b/let-7 signaling pathway in AS (12). Therefore, targeted regulation of pyroptotic endothelial cells is of significance to prevent AS.

Previous studies have reported that lncRNAs and micro RNAs (miRNAs) serve vital roles in cell pyroptosis (13). LncRNAs are composed of more than 200 nucleotides, and a member of the lncRNAs family, MALAT1, has been reported to be associated with pyroptosis in cardiovascular disease. For instance, MALAT1 promoted high glucose-induced pyroptosis of H9c2 cells by competitively binding to miR-141-3p (14). Moreover, up-regulation of MALAT1 aggravates NLRP3-mediated cell pyroptosis in diabetic atherosclerosis (15,16). MALAT1 knockdown significantly decreases high-glucose- induced endothelial and epithelial cell pyroptosis (16,17). However, the effect of MALAT1 on TNF-α-induced pyroptosis of rat aortic endothelial cells (RAOECs) and the underlying mechanisms have been inadequately investigated. miRNAs are composed of 20-24 nucleotides, and their main function is to participate in the regulation of post-transcriptional gene expression (18). Numerous studies have reported that dysregulation of microRNAs, such as miR-30c-5p, leads to the development of AS. Ceolotto *et al* (19) reported the decreased level of miR-30c-5p in microparticles accelerated AS. Moreover, Li *et al* (20) reported that a miR-30c-5p mimic decreased NLRP3-induced endothelial cells pyroptosis by inhibiting forkhead box O3 (FOXO3) expression. However, the effects and precise molecular mechanisms of the MALAT1/miR-30c-5p axis in TNF-α-mediated RAOEC pyroptosis remain to be elucidated.

Connexin 43 (Cx43) is an abundant component in numerous cells of the cardiovascular system. It has been reported that the development of AS is correlated with Cx43 expression (21). Furthermore, a previous study reported that miRNAs serve vital roles in the post-transcriptional regulation of Cx43 expression (22). Yang *et al* (23) reported that miR-1 aggravated arrhythmogenesis via regulation of Cx43. Interestingly, miR-130a also results in cardiac arrhythmias through the downregulation of Cx43 (24). Although MALAT1, miR-30c-5p and Cx43 have been reported to be involved in AS, the mechanisms and interactions still need to be elucidated.

The present study was designed to investigate the functional roles of the MALAT1/miR-30c-5p/Cx43 axis in TNF-α-induced RAOEC pyroptosis and its underlying mechanisms, which could provide new insights into AS treatment.

Materials and methods

Cell culture and treatment. RAOECs (Cell Applications Inc.) and 293T cells (American Type Culture Collection) were cultured in Dulbecco's Modified Eagle Medium (Beijing Solarbio Science & Technology Co., Ltd.) supplemented with 10% fetal bovine serum (Invitrogen; Thermo Fisher Scientific, Inc.), penicillin (100 U/ml) and streptomycin (100 μg/ml) mixture (Beijing Solarbio Science & Technology Co., Ltd.) in a humidified incubator containing 5% CO_2 at 37˚C. RAOECs were exposed to TNF-α (PeproTech, Inc.) at 10 ng/ml for 24 h to induce cell pyroptosis in a humidified incubator containing 5% CO_2 at 37˚C.

The sense and anti-sense sequences for MALAT1, Cx43 and the negative controls were designed by Biomics Biopharma. The sequences for miR-30c-5p mimic (cat. no. miR10000804), miR-30c-5p inhibitor (cat. no. miR20000804), mimic negative control (NC) (cat. no. miR1N0000001-1-1) and inhibitor NC (cat. no. miR2N0000001-1-1) were designed and synthesized by Guangzhou RiboBio Co., Ltd. RAOECs were seeded in six-well plates with $1x10^6$ cells/well and then incubated overnight in a humidified incubator containing 5% CO_2 at 37˚C. 50 nM short interfering RNA (siRNA), 30 nM miR-30c-5p mimic or 100 nM miR-30c-5p inhibitor and mimic NC or inhibitor NC were transfected into RAOECs using riboFECT™ CP Reagent (Guangzhou RiboBio Co., Ltd.) for 24 h followed by 10 ng/ml TNF-α for 24 h in a humidified incubator containing 5% CO_2 at 37˚C. The sequences of purchased siRNA, mimic and inhibitor were presented in Table I.

Reverse transcription-quantitative PCR (RT-qPCR). Total RNA was isolated from RAOECs using TRIzol® reagent (Takara Biotechnology Co., Ltd.). The thermocycling conditions used in RT-qPCR were set as follows: The cDNA synthesis reaction mix was incubated at 25˚C for 5 min and 42˚C for 30 min followed by 85˚C for 5 sec. Then the reaction was terminated at 4˚C. The qPCR reaction mix was incubated at 95˚C for 30 sec for 1 cycle), at 95˚C for 15 sec and at 60˚C for 30 sec for 40 cycles), followed by dissociation. RT-qPCR was performed using Servicebio™ 2xSYBRGreen qPCR Master Mix (Wuhan Servicebio Technology Co., Ltd.) using a CFX Connect™ system (Bio-Rad Laboratories, Inc.). All experiments were performed three times, and the relative gene expression was calculated using the $2^{-\Delta\Delta Cq}$ method (25). U6 was used as an internal control for miR-30c-5p, and GAPDH was used as the internal control for other targets. In the present study, the stem ring method was used for the design of primers for the detection of miR-30c-5p, as the length of mature miRNA is about 20 bp, and the appropriate detection length of RT-qPCR is 80-150 bp. Therefore, it was necessary to add stem-ring structures in the original sequence to extend the miRNA and the miRNA reverse primer was located in in the stem ring, not the miRNA. The primers for miR-30c-5p, MALAT1, U6 and GAPDH were designed and synthetized by Sangon Biotech Co., Ltd. The gap junction protein alpha 1 (GJA1) gene encodes the protein Cx43 and the primer for GJA1 was designed and synthetized by TsingKe Biological Technology. The sequences of the primers were presented in Table II.

Table I. Sequences of siRNAs.

Target	Sequence (5'-3')
siNC	Sense: UUCUCCGAACGUGUCACGU
	Anti-sense: UUUAAGCUGUUUAAGUCAC
siMALAT1-1	Sense: GUGACUUAAACAGCUUAAA
	Anti-sense: UUUAAGCUGUUUAAGUCAC
siMALAT1-2	Sense: GGUAGGUCUGGGUUUACUA
	Anti-sense: UAGUAAACCCAGACCUACC
siMALAT1-3	Sense: GAUUAGUAGUCAAAGCAAA
	Anti-sense: UUUGCUUUGACUACUAAUC
siCx43	Sense: GCAUCGAGCUGUCGAUUAU
	Anti-sense: AUAAUCGACAGCUCGAUGC

siRNA, short interfering RNA; MALAT1, metastasis associated lung adenocarcinoma transcript 1; Cx43, connexin 43; NC, negative control.

Table II. Sequences of primers used for reverse transcription-quantitative PCR

Gene	Sequence (5'-3')
MALAT1	F: CTCACTAAAGGCACCGAAGG
	R: GGCAGAGAAGTTGCTTGTGG
miR-30c-5p	F: GCGCGTGTAAACATCCTACACT
	R: AGTGCAGGGTCCGAGGTATT
Cx43	F: TCTGCCTTTCGCTGTAACACT
	R: GGGCACAGACACGAATATGAT
GAPDH	F: GTCATCAACGGGAAACCCAT
	R: ACGCCAGTAGACTCCACGACAT
U6	F: CTCGCTTCGGCAGCACA
	R: AACGCTTCACGAATTTGCGT

MALAT1, metastasis associated lung adenocarcinoma transcript 1; Cx43, connexin 43; miR, micro RNA; F, forward; R, reverse.

Western blotting. Following experimental treatment, RAOECs were lysed using RIPA lysis buffer (Beyotime Institute of Biotechnology) mixed with phenylmethanesulfonyl fluoride (Beijing Solarbio Science & Technology Co., Ltd.) at a ratio of 1:100. The protein concentration was assessed using a BCA protein assay kit (Applygen Technologies, Inc.). Protein samples of 20 μg/well were loaded and separated using 10 or 12% SDS-PAGE and then transferred onto PVDF membranes (MilliporeSigma). Subsequently, the membranes were blocked using 5% bovine serum albumin (Shanghai Yeasen Biotechnology Co., Ltd.) for 2 h at room temperature, and then incubated with primary antibodies against NLRP3 (1:500; cat. no. 27458-1-AP; Proteintech Group, Inc.), cleaved caspase-1 (1:500; cat. no. sc-398715; Santa Cruz Biotechnology, Inc.), IL-1β (1:500; cat. no. sc-515598; Santa Cruz Biotechnology, Inc.), Cx43 (1:1,000; cat. no. sc-271837; Santa Cruz Biotechnology, Inc.), GSDMD-N (1:1,000; cat. no. YT7991; ImmunoWay Biotechnology Company), ASC (1:1,000; cat. no. YT0365; Immunoway Biotechnology Company) and GAPDH (1:1,000 cat. no. TA802519; OriGene Technologies, Inc.) and β-actin (1:5,000; cat. no. 66009-1-Ig; Proteintech Group, Inc.) overnight at 4°C. After washing 3 times with TBST containing 0.05% Tween-20, the membranes were incubated with peroxidase-conjugated goat anti-rabbit IgG(H+L) (1:8,000; cat. no. 33101ES60; Shanghai Yeasen Biotechnology Co., Ltd.) or peroxidase-conjugated goat anti-mouse IgG(H+L) (1:8,000; cat. no. 33201ES60; Shanghai Yeasen Biotechnology Co., Ltd.) secondary antibodies for 2 h at room temperature. Protein signaling was detected using an enhanced chemiluminescence kit (Abbkine Scientific Co., Ltd.) and analyzed using ImageJ software v1.8.0 (National Institutes of Health). GAPDH was used as the internal control. Each experiment was performed three times.

Lactate dehydrogenase (LDH) release assay. An LDH assay kit (cat. no. C0017; Beyotime Institute of Biotechnology) was used to determine the LDH activity of RAOECs in each group according to the manufacturer's protocols. Briefly, 120 μl cell supernatant, collected by centrifugation at 400 x g for 5 min at room temperature and 60 μl reaction mixture (20 μl lactate, 20 μl 2-p-iodophenyl-3-nitrophenyl tetrazolium chloride and 20 μl diaphorase) were mixed and incubated for 0.5 h at room temperature. A Bio-Rad 680 spectrophotometric microplate reader (Bio-Rad Laboratories, Inc.) was used to quantify the absorbance at 490 nm.

Hoechst 33342/propidium iodide (PI) staining. RAOECs ($1x10^5$ cells/well in 12-well plates) were treated with TNF-α or transfected with different constructs. After washing with PBS, the cells were incubated with 2.5 μl Hoechst 33342 solution and PI (Beyotime Institute of Biotechnology) for 0.5 h in the dark at 4°C. After washing 3 times with PBS, the stained cells were imaged using a DMi8 inverted fluorescence microscope at 200x magnification (Leica Microsystems GmbH).

Dual-luciferase reporter assay. The targets of MALAT1 were predicted using the StarBase (http://starbase.sysu.edu.cn) and BiBiServ2 (http://bibiserv.techfak.uni-bielefeld.de/) databases. Briefly, the gene sequences of MALAT1 (human sequence used as no entry for rat on NCBI) and miR-30c-5p were acquired from NCBI (https://www.ncbi.nlm.nih.gov/) and searched using standard conditions on the BiBiServ2 website. The targets of miR-30c-5p in humans were searched using TargetScan8.0 online. The dual-luciferase reporter assay was performed to evaluate the binding of MALAT1 and miR-30c-5p as well as that of miR-30c-5p and Cx43. Partial sequences of MALAT1 or Cx43 carrying putative wild-type (WT) miR-30c-5p binding sites or mutant (MUT) sites were cloned into the GV272 luciferase vector (Shanghai GeneChem Co., Ltd.) and named MALAT1-WT, MALAT1-MUT, Cx43-WT and Cx43-MUT. Similarly, the CV045 vector containing the renilla luciferase reporter gene was also purchased from Shanghai GeneChem Co., Ltd. The 293T cell line, a powerful tool cell for expressing exogenous genes, is competent to replicate vectors carrying the SV40 region of replication, which has been widely used for retroviral production, gene expression and protein production (26). So 293T cells were co-transfected with 20 pmol miR-30c-5p

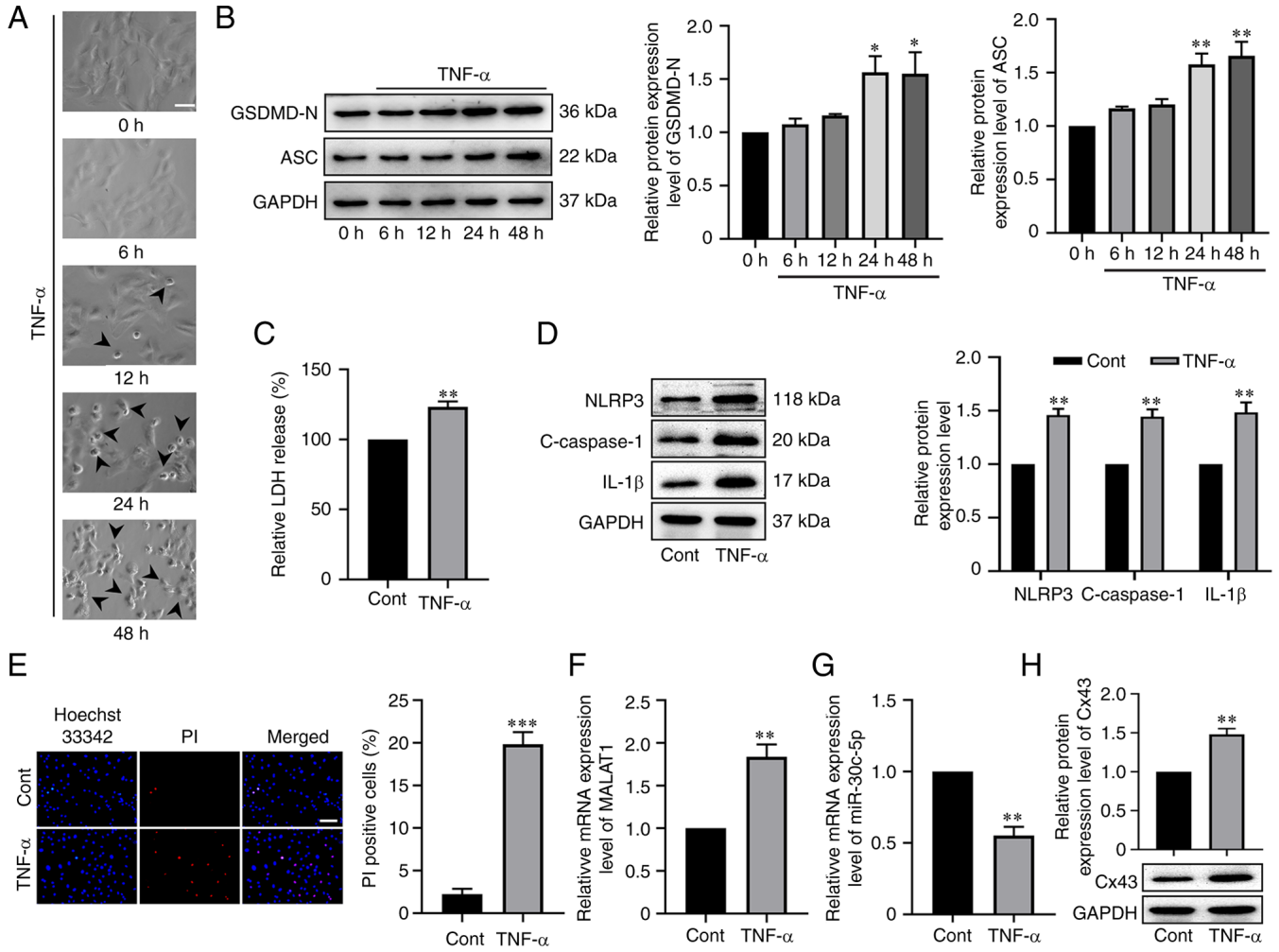

Figure 1. MALAT1 and Cx43 were up-regulated but miR-30c-5p was down-regulated in TNF-α-induced RAOEC pyroptosis. (A) Representative bright-field microscopic images of RAOEC treated with 10 ng/ml TNF-α for 0, 6, 12, 24 and 48 h. The arrowheads (black) indicate pyroptotic cells (scale bar=50 μm). (B) Western blotting was performed to assess the protein expression levels of GSDMD-N and ASC in RAOEC treated with 10 ng/ml TNF-α for 0, 6, 12, 24 and 48 h. (C) A LDH assay kit was used to assess the LDH release of RAOECs. (D) Western blotting was performed to assess the protein expression levels of NLRP3, C-caspase-1 and IL-1β. (E) Hoechst 33342 (blue) and PI (red) double-fluorescent staining of RAOECs, after different treatments, was used to assess pyroptotic cell death (scale bar=100 μm). The mRNA expression levels of (F) MALAT1 and (G) miR-30c-5p and protein expression levels of (H) Cx43 in RAOECs were evaluated using reverse transcription-quantitative PCR and western blotting, respectively. All data are presented as the mean ± SD (n=3). *P<0.05, **P<0.01 and ***P<0.001 vs. Cont. MALAT1, metastasis associated lung adenocarcinoma transcript 1; Cx43, connexin 43; miR, micro RNA; TNF-α, tumor necrosis factor-α; RAOECs, rat aorta endothelial cells; GSDMD-N, N-terminus of gasdermin D; ASC, apoptosis-associated speck-like protein containing a CARD; Cont, control; C-caspase-1, cleaved caspase-1; PI, propidium iodide.

mimic or mimic NC and the constructed vectors (0.5 μg of GV272 plasmid and 50 ng of CV045 plasmid) using Hieff Trans™ Liposomal Transfection Reagent (Shanghai Yeasen Biotechnology Co., Ltd.). After 48 h, firefly and *Renilla* luciferase activities were measured using the dual-luciferase reporter assay system (Shanghai Yeasen Biotechnology Co., Ltd.) according to the manufacturer's protocols.

Statistical analysis. All the experiments in the present study were performed independently at least three times. The data were presented as the mean ± SD. GraphPad Prism software version 8.3.0 (GraphPad Software; Dotmatics) was used for statistical analysis. For comparisons between two groups, the unpaired Student's t-test was performed. For comparisons among multiple groups, one way analysis of variance with Tukey's post hoc test was used. P<0.05 was considered to indicate a statistically significant difference.

Results

Expression of MALAT1 mRNA and Cx43 protein are elevated but miR-30c-5p expression is decreased in TNF-α-mediated RAOEC pyroptosis. To evaluate whether MALAT1 mRNA, and miR-30c-5p and Cx43 protein expression were related to TNF-α-induced RAOEC pyroptosis, first, RAOECs were incubated with 10 ng/ml TNF-α for 0, 6, 12, 24 or 48 h. RAOEC morphology was characterized by large bubbles, which emerged from the plasma membrane at 12 h, and especially at 24 and 48 h (Fig. 1A). Consistently, western blotting results demonstrated that compared with control groups, the protein expression levels of GSDMD-N and ASC were significantly upregulated after RAOEC treatment with TNF-α for 24 and 48 h; however, there was no significant difference between the 24 and 48 h groups (P<0.05, Fig. 1B). Therefore, the RAOEC pyroptosis model which used 10 ng/ml TNF-α for 24 h was

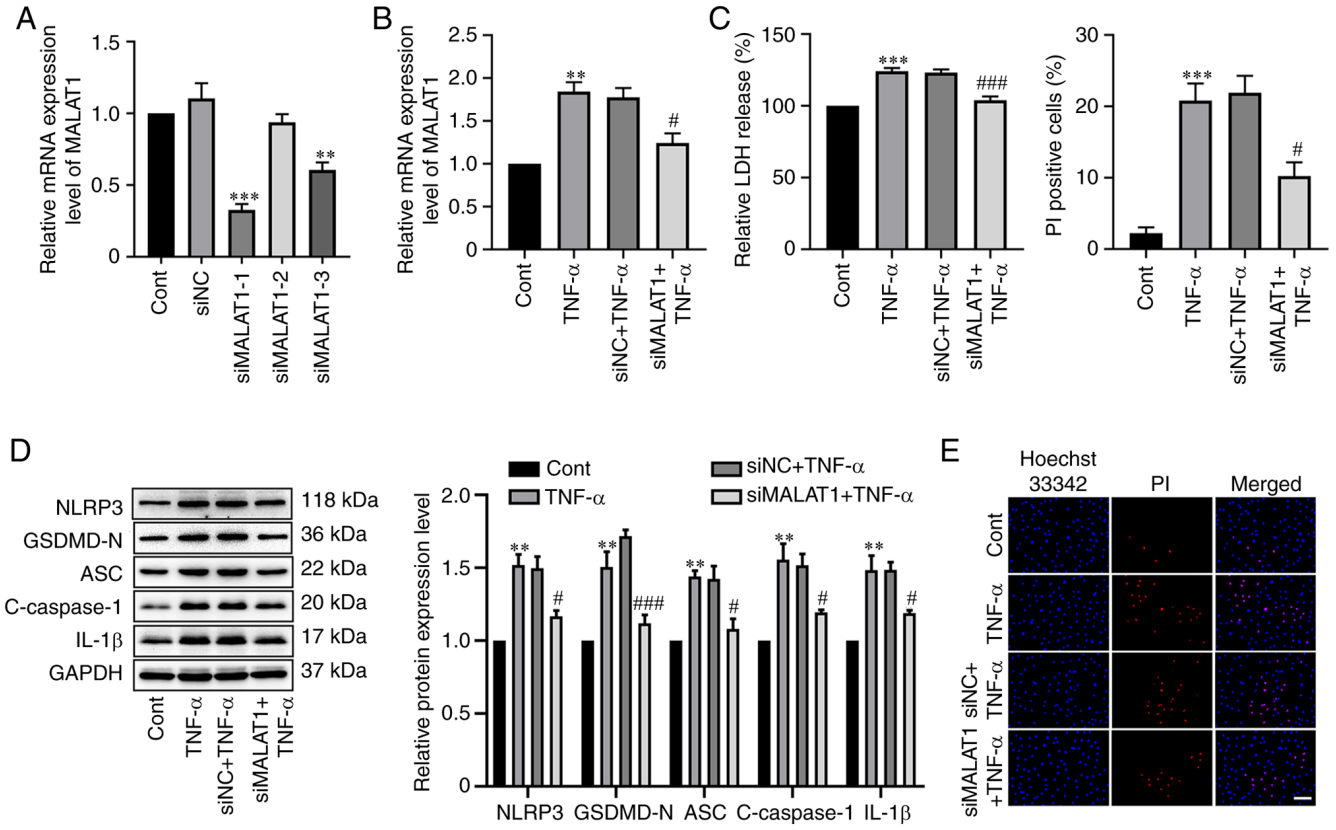

Figure 2. MALAT1 knockdown inhibited TNF-α-induced RAOEC pyroptosis. (A) The mRNA expression level of MALAT1 was evaluated using RT-qPCR in RAOEC with Cont, siNC, or specific siRNAs (siMALAT1-1, siMALAT1-2, siMALAT1-3). **P<0.01 and ***P<0.001 vs. siNC. (B) The mRNA expression level of MALAT1 in RAOECs transfected with siMALAT1 for 24 h and then treated with TNF-α for 24 h was evaluated using RT-qPCR analysis. (C) A LDH assay kit was used to assess LDH release. (D) Western blotting was performed to assess the protein expression levels of NLRP3, GSDMD-N, ASC, C-caspase-1 and IL-1β. (E) Hoechst 33342 (blue) and PI (red) double-fluorescent staining of RAOECs, after different treatments, was used to indicate pyroptotic cell death (scale bar=100 μm). All data are presented as the mean ± SD (n=3). **P<0.01 and ***P<0.001 vs. Cont. $^{\#}$P<0.05 and $^{\#\#\#}$P<0.001 vs. siNC + TNF-α. MALAT1, metastasis associated lung adenocarcinoma transcript 1; TNF-α, tumor necrosis factor-α; RAOECs, rat aorta endothelial cells; siRNA, short interfering RNA; Cont, control; NC, negative control; RT-qPCR, reverse transcription-quantitative PCR; GSDMD-N, N-terminus of gasdermin D; NLRP3, NLR family pyrin domain containing 3; ASC, apoptosis-associated speck-like protein containing a CARD; Cont, control; C-caspase-1, cleaved caspase-1; PI, propidium iodide.

used in the subsequent experiments. Next, cell damage was evaluated by assessing LDH release, which indicated that TNF-α treatment significantly increased LDH release (t=6.031, P=0.0038, Fig. 1C). Furthermore, western blotting was performed to assess the protein expression levels of NLRP3, cleaved caspase-1 and IL-1β in TNF-α-stimulated RAOECs, and the results indicated that NLRP3 (t=7.967, P=0.0013), cleaved caspase-1 (t=6.482, P=0.0029) and IL-1β (t=5.149, P=0.0067) were all significantly upregulated compared with the control (Fig. 1D). Accordingly, it was demonstrated that the percentage of PI-positive cells was significantly elevated in TNF-α-treated RAOECs compared with the control (t=11.35, P=0.0003, Fig. 1E). Interestingly, it was also demonstrated that TNF-α treatment significantly increased the mRNA expression level of MALAT1 (t=5.801, P=0.0044, Fig. 1F) and protein expression level of Cx43 (t=6.512, P=0.0029, Fig. 1G), but significantly reduced the RNA expression level of miR-30c-5p (t=7.352, P=0.0018, Fig. 1H). The aforementioned results indicated that MALAT1, miR-30c-5p and Cx43 could be associated with TNF-α-induced RAOEC pyroptosis.

Knockdown of MALAT1 alleviates TNF-α-mediated RAOEC pyroptosis. To further assess the effect of MALAT1 on TNF-α-mediated RAOEC pyroptosis, three specific siRNAs targeting MALAT1 were designed, and the mRNA expression level of MALAT1 was assessed using RT-qPCR. The results demonstrated a significant reduction in MALAT1 expression in the siMALAT1-1 (P<0.0001) and siMALAT1-3 (P=0.0013) groups compared with the negative control, and siMALAT1-1 was considered the best and so used for subsequent experiments (Fig. 2A). Next, it was demonstrated that knockdown of MALAT1 significantly reversed the elevated mRNA expression level of MALAT1 caused by TNF-α treatment in RAOECs (Fig. 2B). Subsequently, the influence of silencing MALAT1 on TNF-α-induced pyroptosis was assessed using LDH release, pyroptosis-related protein expression levels and the percentage of PI-positive cell numbers. The results demonstrated that the increase in LDH release in TNF-α-stimulated RAOECs was significantly attenuated by MALAT1 knockdown (P=0.0007, Fig. 2C). Moreover, MALAT1 knockdown significantly reversed the up-regulation of NLRP3 (P=0.0161), GSDMD-N (P=0.0007), ASC (P=0.0159), cleaved caspase-1 (P=0.0396) and IL-1β (P=0.0267) protein expression levels in TNF-α-stimulated RAOECs compared with the TNF-α-stimulated negative control (Fig. 2D). Furthermore, the elevation of the number of PI-positive cells induced by TNF-α was significantly suppressed by MALAT1 knockdown (P=0.0135, Fig. 2E). These data indicated that MALAT1

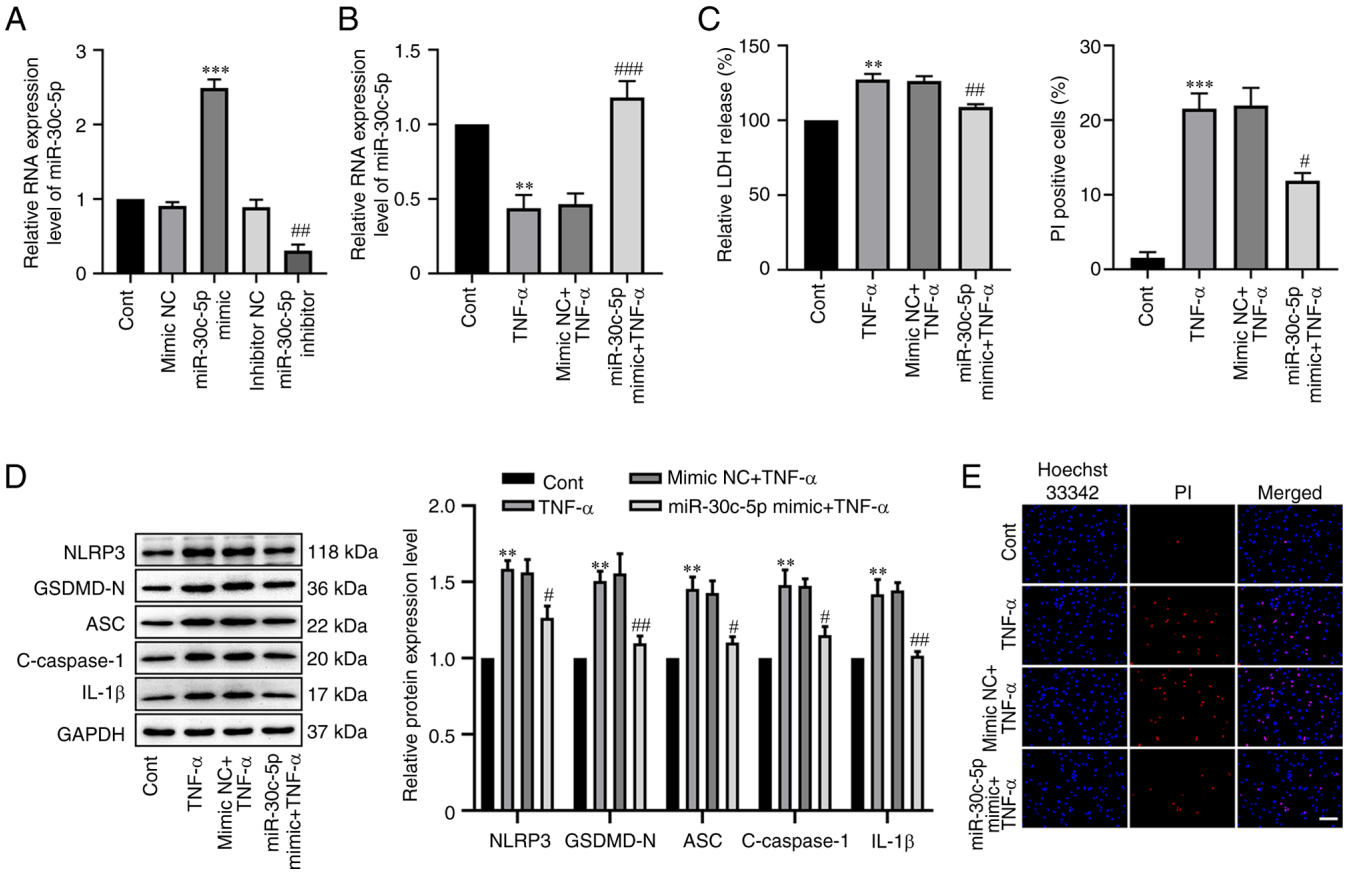

Figure 3. Overexpression of miR-30c-5p reduced TNF-α-mediated RAOEC pyroptosis. (A) The RNA expression level of miR-30c-5p in RAOEC transfected with 30 nM miR-30c-5p mimic or 100 nM miR-30c-5p inhibitor for 48 h was determined using RT-qPCR. (B) The RNA expression level of miR-30c-5p in RAOECs transfected with miR-30c-5p mimic for 24 h and then treated with TNF-α for 24 h was assessed using RT-qPCR. (C) A LDH assay kit was used to assess LDH release. (D) Western blotting was performed to assess the protein expression levels of NLRP3, GSDMD-N, ASC, C-caspase-1 and IL-1β. (E) Hoechst 33342 (blue) and PI (red) double-fluorescent staining of RAOECs, after different treatments, was used to indicate pyroptotic cell death (scale bar=100 μm). All data are presented as the mean ± SD (n=3). **P<0.01 and ***P<0.001 vs. Cont. $^{\#}$P<0.05, $^{\#\#}$P<0.01 and $^{\#\#\#}$P<0.001 vs. mimic NC + TNF-α. RAOECs, rat aorta endothelial cells; TNF-α, tumor necrosis factor-α; miR, micro RNA; RT-qPCR, reverse transcription-quantitative PCR; GSDMD-N, N-terminus of gasdermin D; NLRP3, NLR family pyrin domain containing 3; ASC, apoptosis-associated speck-like protein containing a CARD; Cont, control; C-caspase-1, cleaved caspase-1; PI, propidium iodide.

knockdown was effective in inhibiting TNF-α-induced RAOEC pyroptosis.

miR-30c-5p overexpression attenuates TNF-α-mediated RAOEC pyroptosis. To elucidate the effect of miR-30c-5p in TNF-α-mediated RAOEC pyroptosis, miR-30c-5p overexpression was successfully established which significantly increased miR30c-5p RNA expression levels compared with the negative control (P<0.0001, Fig. 3A). In the present study, it was also demonstrated that the RNA expression level of miR-30c-5p in RAOECs transfected with 100 nM miR-30c-5p inhibitor for 48 h was significantly decreased (P=0.0030). Next, the cells were transfected with miR-30c-5p mimic before treatment with TNF-α. RT-qPCR analysis demonstrated that in the miR-30c-5p mimic + TNF-α group, the level of miR-30c-5p was significantly increased compared with the mimic NC + TNF-α group (P=0.0009, Fig. 3B). Furthermore, compared with the mimic NC + TNF-α group, the miR-30c-5p mimic significantly attenuated LDH release (P=0.0074, Fig. 3C), significantly reduced the increased protein expression levels of NLRP3 (P=0.0408), GSDMD-N (P=0.0016), ASC (P=0.0199), cleaved caspase-1 (P=0.0255) and IL-1β (P=0.0029) (Fig. 3D), and significantly reduced the proportion of PI-positive cells (P=0.0125, Fig. 3E). These results indicated that the overexpression of miR-30c-5p could inhibit TNF-α-mediated RAOEC pyroptosis.

miR-30c-5p is a target of MALAT1 and can target Cx43. Previous studies have reported that lncRNAs function as a competitive endogenous RNAs (ceRNAs) of certain miRNAs to regulate the expression and function of target mRNAs (27). To further elucidate the mechanism by which MALAT1 was involved in TNF-α-induced RAOEC pyroptosis a bioinformatic approach was used to screen the potential targets of MALAT1. Using the StarBase (http://starbase.sysu.edu.cn/) and BiBiServ (http://bibiserv.techfak.uni-bielefeld.de/) database, miR-30c-5p was identified as a potential target gene of MALAT1 (Fig. 4A). Next, to verify the predicted binding sites, a dual-luciferase reporter vector with either the wild-type MALAT1 fragment or the mutant MALAT1 fragment was constructed. The dual-luciferase reporter gene analysis results demonstrated that miR-30c-5p overexpression significantly attenuated the luciferase activity of the MALAT1-WT reporter (P=0.0047), whereas the luciferase activity of MALAT1-MUT

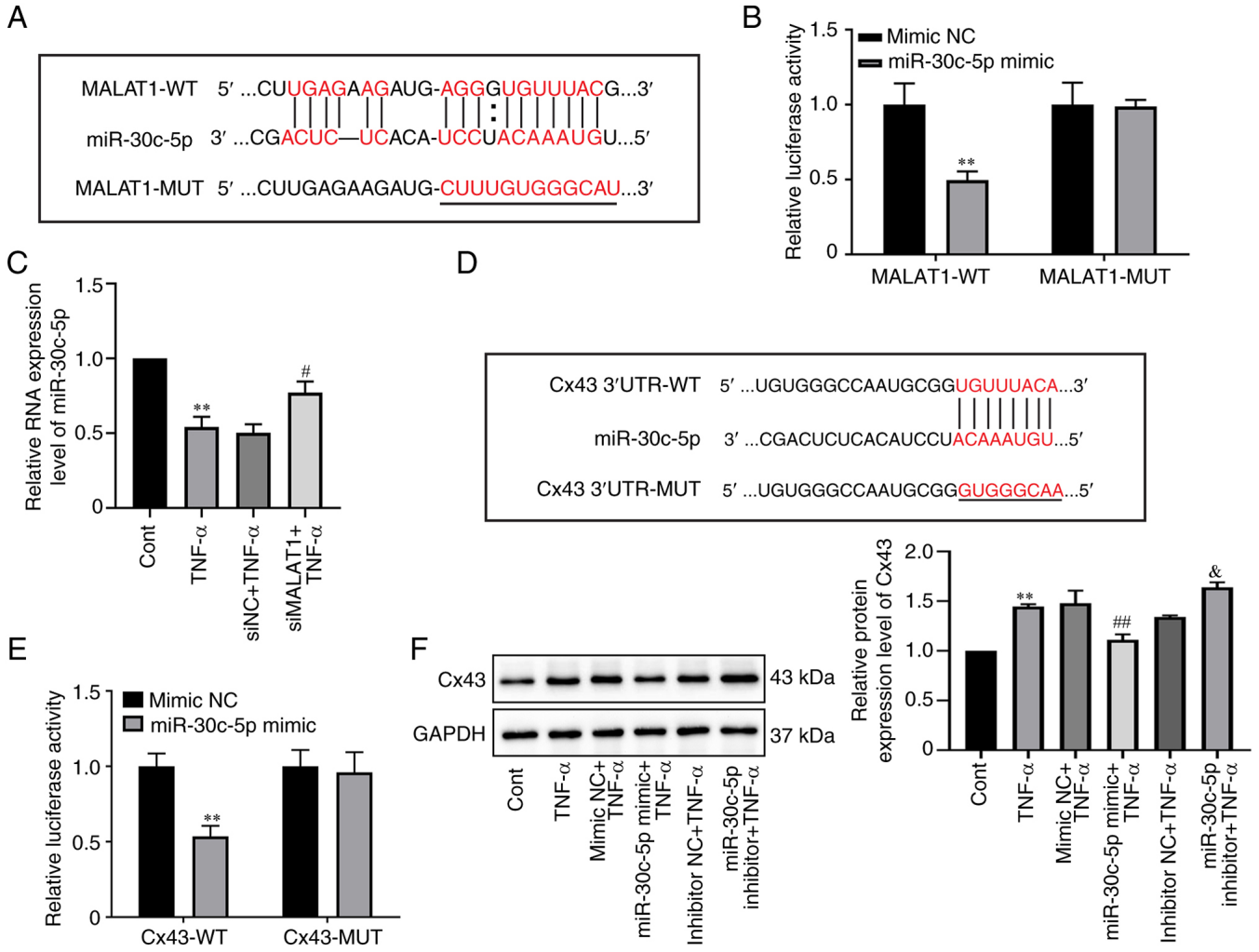

Figure 4. miR-30c-5p is a target of MALAT1 and can target Cx43 in RAOEC. (A) Predicted miR-30c-5p binding sites in the MALAT1-WT and corresponding MALAT1-MUT. The red indicates the binding sites. (B) Luciferase activity in each group was assessed in 293T cells co-transfected with MALAT1-WT or MALAT1-MUT vector and mimic NC or miR-30c-5p mimic. (C) The RNA expression level of miR-30c-5p was assessed in RAOECs transfected with siMALAT1 and then treated with TNF-α, using RT-qPCR. (D) Putative miR-30c-5p binding sites in the 3'UTR of Cx43-WT mRNA and corresponding Cx43-MUT. The red indicates the binding sites. (E) Luciferase activity was evaluated in 293T cells co-transfected with WT or MUT Cx43 reporter and mimic NC or miR-30c-5p mimic. (F) Western blotting was performed to assess the protein expression level of Cx43 in RAOECs transfected with miR-30c-5p mimic or miR-30c-5p inhibitor and then treated with TNF-α. **P<0.01 vs. Cont or mimic NC. $^{\#}$P<0.05 and $^{\#\#}$P<0.01 vs. siNC + TNF-α or mimic NC + TNF-α. $^{\&}$P<0.05 vs. inhibitor NC + TNF-α. All data are presented as the mean ± SD (n=3). RAOECs, rat aorta endothelial cells; Cx43, connexin 43; TNF-α, tumor necrosis factor-α; miR, micro RNA; siRNA, short interfering RNA; RT-qPCR, reverse transcription-quantitative PCR; NC, negative control; WT, wild-type; MUT, mutant.

reporter demonstrated no apparent change (Fig. 4B), which indicated a specific interaction between miR-30c-5p and MALAT1. Furthermore, the RNA expression level of miR-30c-5p was significantly elevated by MALAT1 knockdown compared with the negative control as shown using RT-qPCR analysis (P=0.0430, Fig. 4C). These demonstrated that miR-30c-5p was a target of MALAT1 and was negatively regulated by MALAT1.

Similarly, it was demonstrated that the 3'UTR of Cx43 contained certain miR-30c-5p binding sites according to the TargetScan online software (Fig. 4D). To further confirm the predicted binding sites, a dual-luciferase reporter vector with either the wild-type 3'UTR or mutant 3'UTR of Cx43 was constructed. The results demonstrated that the miR-30c-5p mimic significantly decreased the luciferase activity of the Cx43-WT reporter (P=0.0019) in 293T cells, but had no significant effect on the Cx43-MUT reporter (Fig. 4E). Moreover, compared with the mimic NC + TNF-α groups, the protein expression level of Cx43 was significantly decreased in the miR-30c-5p mimic + TNF-α groups in RAOECs (P=0.0099), whereas compared with the inhibitor NC + TNF-α groups, the protein expression level of Cx43 was significantly increased in the miR-30c-5p inhibitor + TNF-α group (P=0.0393, Fig. 4F). The above results indicated the negative regulatory effect of miR-30c-5p on Cx43 expression in TNF-α-treated RAOECs.

Cx43 downregulation attenuated TNF-α-mediated RAOEC pyroptosis. To further analyze the effect of Cx43 on TNF-α-induced RAOEC pyroptosis, RAOECs were transfected with 50 nM Cx43 siRNA and then stimulated using TNF-α. RT-qPCR and western blotting analysis demonstrated that Cx43 siRNA transfection significantly suppressed the mRNA (P=0.0149) and protein (P=0.0297) expression levels of Cx43 in TNF-α-treated RAOECs compared with the

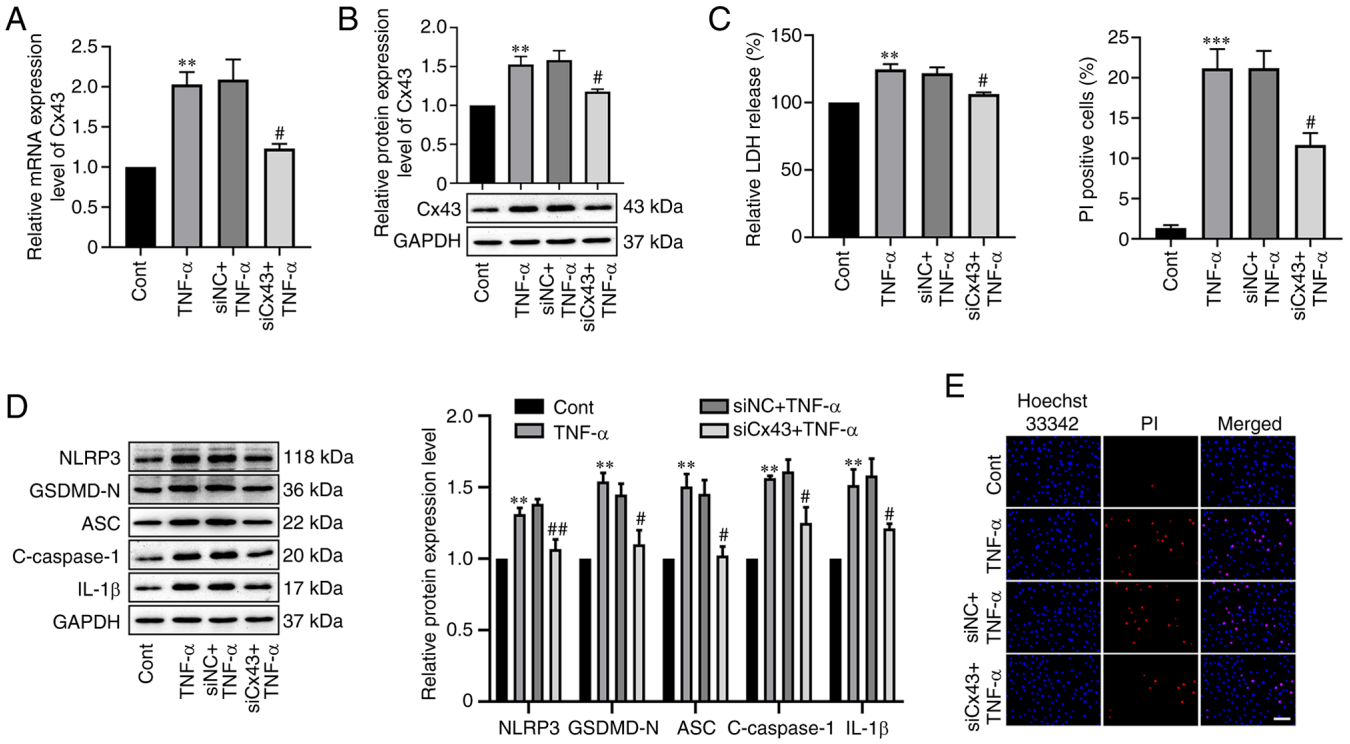

Figure 5. Cx43 knockdown alleviated TNF-α-induced RAOEC pyroptosis. (A) The mRNA expression level of Cx43 in RAOECs transfected with siCx43 for 24 h and then treated with TNF-α for 24 h was assessed using RT-qPCR. (B) Western blotting was performed to assess the protein expression level of Cx43 in RAOEC transfected with siMALAT1 for 24 h and then treated with TNF-α for 24 h. (C) A LDH assay kit was used to assess LDH release. (D) Western blotting was performed to assess the protein expression levels of NLRP3, GSDMD-N, ASC, C-caspase-1 and IL-1β. (E) Hoechst 33342 (blue) and PI (red) double-fluorescent staining of RAOECs, after different treatments, was used to assess pyroptotic cell death (scale bar=100 μm). All data are presented as the mean ± SD (n=3). **P<0.01 and ***P<0.001 vs. Cont. $^{\#}$P<0.05 and $^{\#\#}$P<0.01 vs. siNC + TNF-α. RAOECs, rat aorta endothelial cells; Cx43, connexin 43; TNF-α, tumor necrosis factor-α; siRNA, short interfering RNA; RT-qPCR, reverse transcription-quantitative PCR; NC, negative control; GSDMD-N, N-terminus of gasdermin D; NLRP3, NLR family pyrin domain containing 3; ASC, apoptosis-associated speck-like protein containing a CARD; Cont, control; C-caspase-1, cleaved caspase-1; PI, propidium iodide.

negative control (Fig. 5A and B). Moreover, compared with the siNC + TNF-α group, silencing of Cx43 significantly reduced LDH release (P=0.0265, Fig. 5C). Furthermore, the significantly increased levels of NLRP3 (P=0.0044), GSDMD-N (P=0.0310), ASC (P=0.0129), cleaved caspase-1 (P=0.0279) and IL-1β (P=0.0493) induced by TNF-α were significantly reduced by Cx43 knockdown (Fig. 5D). Downregulation of Cx43 significantly reduced the proportion of PI-positive cells stimulated by TNF-α compared with the negative control (P=0.0221, Fig. 5E). These results demonstrated that knockdown of Cx43 attenuated TNF-α-induced RAOEC pyroptosis.

MALAT1 knockdown inhibited TNF-α-induced RAOEC pyroptosis via miR-30c-5p/Cx43 axis. To further elucidate whether MALAT1 could inhibit TNF-α-induced RAOEC pyroptosis through the miR-30c-5p/Cx43 axis. RAOECs were transfected with siMALAT1 (or siNC) alone or together with miR-30c-5p inhibitor (or inhibitor NC) before treatment with TNF-α. Western blotting demonstrated that the protein expression level of Cx43 was significantly decreased by siMALAT1 transfection in TNF-α-induced RAOECs (P=0.0374), but this effect was significantly weakened by co-transfection of siMALAT1 with miR-30c-5p inhibitor (P=0.0456, Fig. 6A). Similarly, MALAT1 knockdown significantly decreased LDH release in TNF-α-induced RAOECs (P=0.0011), which was significantly reversed by co-transfection of siMALAT1 and miR-30c-5p inhibitor (P=0.0229, Fig. 6B). Furthermore, it was demonstrated that siMALAT1 significantly decreased the protein expression levels of NLRP3 (P=0.0100), GSDMD-N (P=0.0066), ASC (P=0.0115), cleaved caspase-1 (P=0.0041) and IL-1β (P=0.0304) (Fig. 6C), and the percentage of PI-positive cells (P=0.0008, Fig. 6D) compared with the negative control. However, co-transfection of siMALAT1 and miR-30c-5p inhibitor significantly attenuated the decrease in the protein expression levels of NLRP3 (P=0.0232), GSDMD-N (P=0.0421), ASC (P=0.0342), cleaved caspase-1 (P=0.0157) and IL-1β (P=0.0363), and the percentage of PI-positive cells (P=0.0174). The aforementioned results strongly indicated that miR-30c-5p inhibitor could reverse the inhibitory effects of siMALAT1 on TNF-α-induced RAOEC pyroptosis. Hence, it was concluded that MALAT1 served a vital role in TNF-α-induced RAOEC pyroptosis by the regulation of Cx43 expression by sponging miR-30c-5p.

Discussion

Endothelial dysfunction is considered to be an early step in the development of AS (28). In recent decades, anti-inflammatory agents have become an important therapeutic approach for AS (29-31). Pyroptosis is the result of inflammasome activation and has been reported to be closely involved in AS. However,

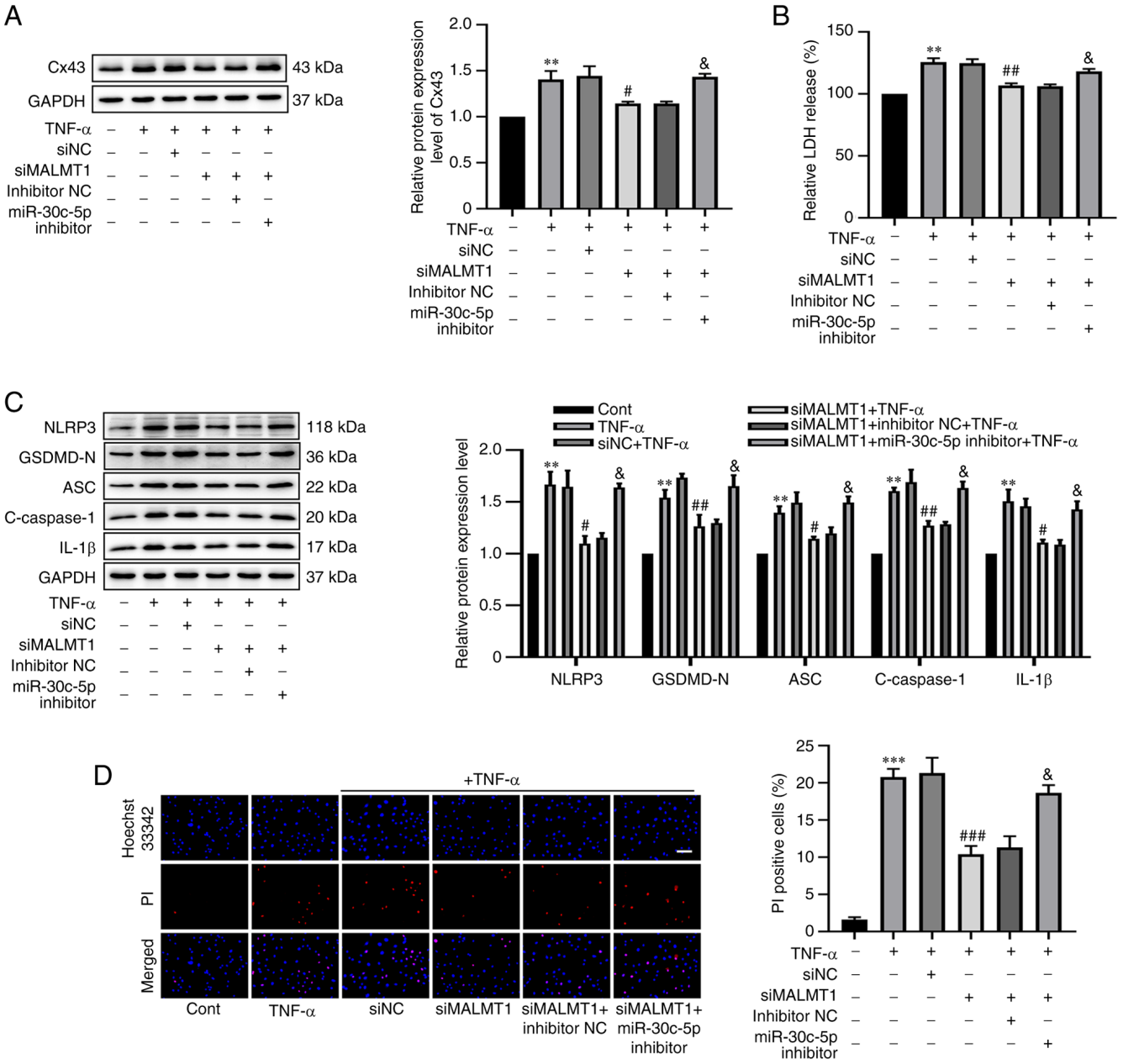

Figure 6. Knockdown of MALAT1 reduced Cx43 expression through targeting miR-30c-5p to decrease TNF-α-induced RAOEC pyroptosis. RAOECs were transfected with siNC, siMALAT1, siMALAT1 + inhibitor NC or siMALAT1 + miR-30c-5p inhibitor and then treated with TNF-α. (A) The protein expression level of Cx43 was assessed using western blotting. (B) A LDH assay kit was used to assess LDH release. (C) Western blotting was performed to assess the protein expression levels of NLRP3, GSDMD-N, ASC, C-caspase-1 and IL-1β. (D) Hoechst 33342 (blue) and PI (red) double-fluorescent staining of RAOECs, after different treatments, was used to assess pyroptotic cell death (scale bar=100 μm). All data are presented as mean ± SD (n=3). **P<0.01 and ***P<0.001 vs. Cont. $^{\#}$P<0.05, $^{\#\#}$P<0.01 and $^{\#\#\#}$P<0.001 vs. siNC + TNF-α. $^{\&}$P<0.05 vs. siMALAT1 + inhibitor NC + TNF-α. MALAT1, metastasis associated lung adenocarcinoma transcript 1; RAOECs, rat aorta endothelial cells; Cx43, connexin 43; TNF-α, tumor necrosis factor-α; siRNA, short interfering RNA; RT-qPCR, reverse transcription-quantitative PCR; NC, negative control; GSDMD-N, N-terminus of gasdermin D; NLRP3, NLR family pyrin domain containing 3; ASC, apoptosis-associated speck-like protein containing a CARD; Cont, control; C-caspase-1, cleaved caspase-1; PI, propidium iodide.

the molecular mechanism has not yet been fully elucidated. Therefore, the present study assessed the upstream regulatory mechanism of pyroptosis. Previous studies have reported that cells incubated with certain concentrations of TNF-α for different time points will exhibit varied effects, including pyroptosis, apoptosis and exhaustion (32-34). Furthermore, accumulated evidence has indicated that TNF-α is a critical inflammatory factor that can increase pyroptosis-related protein expression (32). For instance, Wang *et al* (35) reported that a decrease in TNF-α could attenuate the process of pyroptosis. Moreover, ghrelin reduces pyroptosis, apoptosis and autophagy in human hepatocytes treated with TNF-α (32). In the present study, it was demonstrated that treatment with 10 ng/ml TNF-α for 24 h resulted in a typical pyroptotic morphology and increase in LDH release, pyroptosis-related protein expression and the proportion of PI-positive cells in RAOECs, which suggested that TNF-α induced RAOEC pyroptosis. However, whether treatment with 10 ng/ml TNF-α for 24 h impacts cells exhaustion and apoptosis requires further evaluation.

Recent studies have reported that MALAT1 is of significance in the regulation of pyroptosis in numerous cell types through direct or indirect pathways. For example, MALAT1 is considered a ceRNA that regulates the level of NLRP3 by downregulating miR-22 in high glucose-induced human endothelial cell pyroptosis (17). Similarly, knockdown of MALAT1 up-regulated miR-558 by decreasing GSDMD to inhibit inflammation, apoptosis and pyroptosis of chondrocytes in ankylosing spondylitis (36). Furthermore, MALAT1 knockdown significantly decreased the inflammation and pyroptosis of macrophages (37). In agreement with the aforementioned previous studies, in the present study, MALAT1 was significantly upregulated in TNF-α-induced RAOEC pyroptosis, whereas knockdown of MALAT1 significantly attenuated this effect. The demonstrated that MALAT1 was involved in TNF-α-induced RAOEC pyroptosis was an innovation of the present study. LncRNAs are reported to function as a 'sponge' or 'ceRNA', thus regulating miRNA expression (38). In the present study, it was demonstrated that TNF-α treatment significantly decreased the miR-30c-5p expression level in RAOECs. Previous studies have indicated that miR-30 family members, especially miR-30c-5p, act as protective factors in numerous solid tumors, such as non-small cell lung (39), pancreatic (40) and liver (41) tumors. Recently, miR-30c-5p has been reported to be closely associated with the development of cardiovascular diseases, including AS (19), diabetic nephropathy (42) and myocardial ischemia-reperfusion injury (43). Furthermore, Li *et al* (20) reported that the level of miR-30c-5p was decreased in ox-LDL-mediated endothelial cells, and that overexpression of miR-30c-5p suppressed the endothelial cell pyroptosis triggered by ox-LDL. Consistent with these findings, the present study also demonstrated that overexpression of miR-30c-5p attenuated TNF-α-induced RAOEC pyroptosis. Huntzinger *et al* (44) reported that microRNAs could induce the translational repression of targeted mRNA (relatively common in plants) or the degradation of targeted mRNA (relatively common in mammals). Subsequently, by performing a bioinformatic analysis, Pubmed search and dual-luciferase reporter assay, the potential interaction between MALAT1 and miR-30c-5p was demonstrated. Similarly, based on prediction using the TargetScan website, it was hypothesized that Cx43 might be a target gene for miR-30c-5p, which was involved in TNF-α-induced RAOEC pyroptosis. Furthermore, the dual-luciferase reporter assays significantly demonstrated that Cx43 was a direct target of miR-30c-5p, and was negatively regulated by miR-30c-5p, in accordance with the results that TNF-α treatment downregulated miR-30c-5p and upregulated Cx43 expression. Cx43 is a transmembrane protein whose main function is to form a gap junction that allows the exchange of molecules that are smaller than 1.2 kDa, such as small molecules (ATP, GTP, etc.), ions (K^+, Ca^{2+}, etc.) and secondary messengers (cAMP, cGMP, etc.) (45). Cx43 can function in various forms, namely, in gap junctions, in hemichannels or by itself, and it is involved in all cell cycle stages, such as growth, differentiation and apoptosis (46). Increasing evidence indicates that Cx43 is also closely associated with the development of cardiovascular diseases, especially AS (47,48). Nevertheless, the underlying mechanisms are not clearly defined. Morel *et al* (49) reported that decreased levels of Cx43 served a protective role in the development of atherosclerotic lesions in mice. Moreover, accumulating research has demonstrated that Cx43 is closely related to inflammasome activation and Cx43 gap junctions or hemichannels allowing communication between the intracellular and extracellular milieu (50,51). However, Cx43 can regulate immune cell activation, which is influenced by inflammasome activation (52). Similarly, Cx43 is associated with NLRP3 inflammasome activation in nerve pain (53), retinal disease (54) and chronic kidney disease (55). Zhang *et al* (56) reported that bioactive glass suppressed endothelial cell pyroptosis via decrease of the levels of Cx43 and reactive oxygen species. Blocking Cx43 alleviated renal fibrosis by decreasing the pyroptosis of macrophages (57). Consistently, the results of the present study demonstrated that Cx43 expression was markedly elevated in TNF-α-induced RAOECs and knockdown of Cx43 attenuated TNF-α-induced RAOEC pyroptosis, which indicated that Cx43 was related to the TNF-α-induced RAOEC pyroptosis.

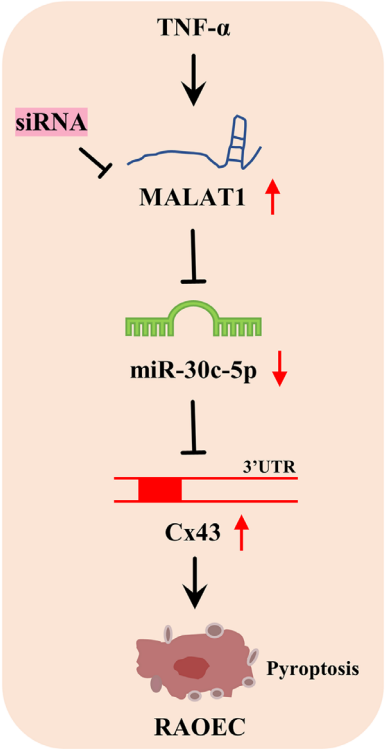

Figure 7. Knockdown of the long non-coding RNA MALAT1 ameliorates TNF-α-mediated RAOEC pyroptosis via the miR-30c-5p/Cx43 axis. MALAT1, metastasis associated lung adenocarcinoma transcript 1; RAOECs, rat aorta endothelial cells; Cx43, connexin 43; TNF-α, tumor necrosis factor-α; siRNA, short interfering RNA; miR, micro RNA.

The results of the present study demonstrated that MALAT1 could indirectly regulate the level of Cx43 by targeting miR-30c-5p. Western blotting analysis demonstrated that MALAT1 knockdown significantly reduced Cx43 expression, while miR-30c-5p inhibition significantly reversed this effect. Furthermore, miR-30c-5p inhibition suppressed the MALAT1 knockdown-induced inhibitory effect on pyroptosis in TNF-α-induced RAOEC. The present study demonstrated that MALAT1 could regulate Cx43 expression in TNF-α-induced RAOEC pyroptosis by sponging miR-30c-5p.

To the best of our knowledge, the present study is the first to demonstrate that MALAT1 regulates TNF-α-induced

RAOEC pyroptosis via the miR-30c-5p/Cx43 axis, which further elucidates the pathogenesis of AS. However, certain limitations due to the complexity and diversity of the regulation between molecules in the cells used in the present study need to be taken into consideration in the future. For example, the effects of the MALAT1/miR-30c-5p/Cx43 axis in RAOEC pyroptosis in AS need to be further assessed *in vivo*. Secondly, in the present study, bioinformatic analyses demonstrated that miR-30c-5p has a broadly conserved binding site with lncRNA MALAT1, and it is known that miR-30c-5p is closely related to endothelial cells injury in AS (20). Furthermore, previous studies have reported that miR-30c-5p was a target gene of MALAT1 (58-60). However, the relationship between miRNA and lncRNA is very complex, and it is not currently possible to rule out other possible targets of MALAT1. Therefore, more molecules, such as miR-24, miR-204-5p and miR-26b-5p, need to be further evaluated in future. Finally, the present study was at the early stage and mainly assessed the role and underlying mechanisms of MALAT1 in TNF-α-mediated endothelial cell pyroptosis. Further studies are required to elucidate if manipulation of these genes impacted tube formation and angiogenesis of endothelial cells *in vitro* and *in vivo*.

In summary, MALAT1 was demonstrated to be significantly elevated in TNF-α-treated RAOECs and targeted miR-30c-5p expression. As a target gene of miR-30c-5p, Cx43 was significantly elevated in TNF-α-induced RAOECs. Knockdown of MALAT1 could inhibit the TNF-α-induced pyroptosis of RAOECs by indirectly downregulating Cx43 via the targeting of miR-30c-5p expression (Fig. 7), which suggested that MALAT1 may be a potential therapeutic target for the treatment of AS.

Acknowledgements

Not applicable.

Funding

This work was supported by the National Natural Science Foundation of China (grant no. 82160686), the Key Program of the Natural Science Foundation of Jiangxi Province (grant no. 20202ACB206001), the Key Research and Development Program of Jiangxi Province (grant no. 20192BBG70012), and the Research Fund for Key Laboratory of Drug Targets and Drug Screening of Jiangxi Province (grant no. 20171BCD40007).

Availability of data and materials

The datasets used and/or analyzed during the current study are available from the corresponding author upon reasonable request.

Authors' contributions

ZJY and RL were responsible for conceptualization, the methodology, data curation and writing the original draft of the manuscript. XJH was responsible for conceptualization, formal analysis and reviewing the manuscript. CLQ and LHL were responsible for the methodology and data analysis. GLD, ZQL and YL were responsible for the methodology and data interpretation. LPJ was responsible for conceptualization, the methodology, formal analysis, reviewing the manuscript, funding acquisition and provided supervision. Z-JY and RL confirm the authenticity of all the raw data.

Ethics approval and consent for publication

Not applicable.

Patient consent for publication

Not applicable.

Competing interests

The authors declare that they have no competing interests.

References

1. Li Y, Zhang L, Ren P, Yang Y, Li S, Qin X, Zhang M, Zhou M and Liu W: Qing-Xue-Xiao-Zhi formula attenuates atherosclerosis by inhibiting macrophage lipid accumulation and inflammatory response via TLR4/MyD88/NF-κB pathway regulation. Phytomedicine 93: 153812, 2021.
2. Libby P: Inflammation during the life cycle of the atherosclerotic plaque. Cardiovasc Res 117: 2525-2536, 2021.
3. Li M, Wang ZW, Fang LJ, Cheng SQ, Wang X and Liu NF: Programmed cell death in atherosclerosis and vascular calcification. Cell Death Dis 13: 467, 2022.
4. Qian Z, Zhao Y, Wan C, Deng Y, Zhuang Y, Xu Y, Zhu Y, Lu S and Bao Z: Pyroptosis in the initiation and progression of atherosclerosis. Front Pharmacol 12: 652963, 2021.
5. He X, Fan X, Bai B, Lu N, Zhang S and Zhang L: Pyroptosis is a critical immune-inflammatory response involved in atherosclerosis. Pharmacol Res 165: 105447, 2021.
6. Wang Q, Wu J, Zeng Y, Chen K, Wang C, Yang S, Sun N, Chen H, Duan K and Zeng G: Pyroptosis: A pro-inflammatory type of cell death in cardiovascular disease. Clin Chim Acta 510: 62-72, 2020.
7. Zhang Y, Jiao Y, Li X, Gao S, Zhou N, Duan J and Zhang M: Pyroptosis: A new insight into eye disease therapy. Front Pharmacol 12: 797110, 2021.
8. Burdette BE, Esparza AN, Zhu H and Wang S: Gasdermin D in pyroptosis. Acta Pharm Sin B 11: 2768-2782, 2021.
9. He B, Nie Q, Wang F, Han Y, Yang B, Sun M, Fan X, Ye Z, Liu P and Wen J: Role of pyroptosis in atherosclerosis and its therapeutic implications. J Cell Physiol 236: 7159-7175, 2021.
10. Yao F, Jin Z, Zheng Z, Lv X, Ren L, Yang J, Chen D, Wang B, Yang W, Chen L, *et al*: HDAC11 promotes both NLRP3/caspase-1/GSDMD and caspase-3/GSDME pathways causing pyroptosis via ERG in vascular endothelial cells. Cell Death Discov 8: 112, 2022.
11. Yao F, Jin Z, Lv X, Zheng Z, Gao H, Deng Y, Liu Y, Chen L, Wang W, He J, *et al*: Hydroxytyrosol acetate inhibits vascular endothelial cell pyroptosis via the HDAC11 signaling pathway in atherosclerosis. Front Pharmacol 12: 656272, 2021.
12. Yao F, Lv X, Jin Z, Chen D, Zheng Z, Yang J, Ren L, Wang B, Wang W, He J, *et al*: Sirt6 inhibits vascular endothelial cell pyroptosis by regulation of the Lin28b/let-7 pathway in atherosclerosis. Int Immunopharmacol 110: 109056, 2022.
13. Gao J, Chen X, Wei P, Wang Y, Li P and Shao K: Regulation of pyroptosis in cardiovascular pathologies: Role of noncoding RNAs. Mol Ther Nucleic Acids 25: 220-236, 2021.
14. Wu A, Sun W and Mou F: lncRNA-MALAT1 promotes high glucose-induced H9C2 cardiomyocyte pyroptosis by downregulating miR-141-3p expression. Mol Med Rep 23: 259, 2021.
15. Han Y, Qiu H, Pei X, Fan Y, Tian H and Geng J: Low-dose sinapic acid abates the pyroptosis of macrophages by downregulation of lncRNA-MALAT1 in rats with diabetic atherosclerosis. J Cardiovasc Pharmacol 71: 104-112, 2018.
16. Li X, Zeng L, Cao C, Lu C, Lian W, Han J, Zhang X, Zhang J, Tang T and Li M: Long noncoding RNA MALAT1 regulates renal tubular epithelial pyroptosis by modulated miR-23c targeting of ELAVL1 in diabetic nephropathy. Exp Cell Res 350: 327-335, 2017.

17. Song Y, Yang L, Guo R, Lu N, Shi Y and Wang X: Long noncoding RNA MALAT1 promotes high glucose-induced human endothelial cells pyroptosis by affecting NLRP3 expression through competitively binding miR-22. Biochem Biophys Res Commun 509: 359-366, 2019.
18. Rahimian P and He JJ: HIV-1 tat-shortened neurite outgrowth through regulation of microRNA-132 and its target gene expression. J Neuroinflammation 13: 247, 2016.
19. Ceolotto G, Giannella A, Albiero M, Kuppusamy M, Radu C, Simioni P, Garlaschelli K, Baragetti A, Catapano AL, Iori E, *et al*: miR-30c-5p regulates macrophage-mediated inflammation and pro-atherosclerosis pathways. Cardiovasc Res 114: 1908, 2018.
20. Li P, Zhong X, Li J, Liu H, Ma X, He R and Zhao Y: MicroRNA-30c-5p inhibits NLRP3 inflammasome-mediated endothelial cell pyroptosis through FOXO3 down-regulation in atherosclerosis. Biochem Biophys Res Commun 503: 2833-2840, 2018.
21. Morel S, Burnier L and Kwak BR: Connexins participate in the initiation and progression of atherosclerosis. Semin Immunopathol 31: 49-61, 2009.
22. Klotz LO: Posttranscriptional regulation of connexin-43 expression. Arch Biochem Biophys 524: 23-29, 2012.
23. Yang B, Lin H, Xiao J, Lu Y, Luo X, Li B, Zhang Y, Xu C, Bai Y, Wang H, *et al*: The muscle-specific microRNA miR-1 regulates cardiac arrhythmogenic potential by targeting GJA1 and KCNJ2. Nat Med 13: 486-491, 2007.
24. Osbourne A, Calway T, Broman M, McSharry S, Earley J and Kim GH: Downregulation of connexin43 by microRNA-130a in cardiomyocytes results in cardiac arrhythmias. J Mol Cell Cardiol 74: 53-63, 2014.
25. Livak KJ and Schmittgen TD: Analysis of relative gene expression data using real-time quantitative PCR and the 2(-Delta Delta C(T)) method. Methods 25: 402-408, 2001.
26. Reus JB, Trivino-Soto GS, Wu LI, Kokott K and Lim ES: SV40 large T antigen is not responsible for the Loss of STING in 293T cells but can inhibit cGAS-STING interferon induction. Viruses 12: 137, 2020.
27. Wang Y, Zeng X, Wang N, Zhao W, Zhang X, Teng S, Zhang Y and Lu Z: Long noncoding RNA DANCR, working as a competitive endogenous RNA, promotes ROCK1-mediated proliferation and metastasis via decoying of miR-335-5p and miR-1972 in osteosarcoma. Mol Cancer 17: 89, 2018.
28. Milutinović A, Šuput D and Zorc-Pleskovič R: Pathogenesis of atherosclerosis in the tunica intima, media, and adventitia of coronary arteries: An updated review. Bosn J Basic Med Sci 20: 21-30, 2020.
29. Sitia S, Tomasoni L, Atzeni F, Ambrosio G, Cordiano C, Catapano A, Tramontana S, Perticone F, Naccarato P, Camici P, *et al*: From endothelial dysfunction to atherosclerosis. Autoimmun Rev 9: 830-834, 2010.
30. Xu S, Ilyas I, Little PJ, Li H, Kamato D, Zheng X, Luo S, Li Z, Liu P, Han J, *et al*: Endothelial dysfunction in atherosclerotic cardiovascular diseases and beyond: From mechanism to pharmacotherapies. Pharmacol Rev 73: 924-967, 2021.
31. Raggi P, Genest J, Giles JT, Rayner KJ, Dwivedi G, Beanlands RS and Gupta M: Role of inflammation in the pathogenesis of atherosclerosis and therapeutic interventions. Atherosclerosis 276: 98-108, 2018.
32. Ezquerro S, Mocha F, Frühbeck G, Guzmán-Ruiz R, Valentí V, Mugueta C, Becerril S, Catalán V, Gómez-Ambrosi J, Silva C, *et al*: Ghrelin reduces TNF-α-induced human hepatocyte apoptosis, autophagy, and pyroptosis: Role in obesity-associated NAFLD. J Clin Endocrinol Metab 104: 21-37, 2019.
33. Liu Y and Tie L: Apolipoprotein M and sphingosine-1-phosphate complex alleviates TNF-α-induced endothelial cell injury and inflammation through PI3K/AKT signaling pathway. BMC Cardiovasc Disord 19: 279, 2019.
34. Jing ZT, Liu W, Xue CR, Wu SX, Chen WN, Lin XJ and Lin X: AKT activator SC79 protects hepatocytes from TNF-α-mediated apoptosis and alleviates d-Gal/LPS-induced liver injury. Am J Physiol Gastrointest Liver Physiol 316: G387-G396, 2019.
35. Wang Y, Zhang H, Chen Q, Jiao F, Shi C, Pei M, Lv J, Zhang H, Wang L and Gong Z: TNF-α/HMGB1 inflammation signalling pathway regulates pyroptosis during liver failure and acute kidney injury. Cell Prolif 53: e12829, 2020.
36. Chen W, Wang F, Wang J, Chen F and Chen T: The molecular mechanism of long non-coding RNA MALAT1-mediated regulation of chondrocyte pyroptosis in ankylosing spondylitis. Mol Cells 45: 365-375, 2022.
37. Shu B, Zhou YX, Li H, Zhang RZ, He C and Yang X: The METTL3/MALAT1/PTBP1/USP8/TAK1 axis promotes pyroptosis and M1 polarization of macrophages and contributes to liver fibrosis. Cell Death Discov 7: 368, 2021.
38. Kato M, Wang M, Chen Z, Bhatt K, Oh HJ, Lanting L, Deshpande S, Jia Y, Lai JY, O'Connor CL, *et al*: An endoplasmic reticulum stress-regulated lncRNA hosting a microRNA megacluster induces early features of diabetic nephropathy. Nat Commun 7: 12864, 2016.
39. Zhou Y, Shi H, Du Y, Zhao G, Wang X, Li Q, Liu J, Ye L, Shen Z, Guo Y and Huang Y: lncRNA DLEU2 modulates cell proliferation and invasion of non-small cell lung cancer by regulating miR-30c-5p/SOX9 axis. Aging (Albany NY) 11: 7386-7401, 2019.
40. Tanaka T, Okada R, Hozaka Y, Wada M, Moriya S, Satake S, Idichi T, Kurahara H, Ohtsuka T and Seki N: Molecular pathogenesis of pancreatic ductal adenocarcinoma: Impact of miR-30c-5p and miR-30c-2-3p regulation on oncogenic genes. Cancers (Basel) 12: 2731, 2020.
41. He Z, Tian M and Fu X: Reduced expression of miR-30c-5p promotes hepatocellular carcinoma progression by targeting RAB32. Mol Ther Nucleic Acids 26: 603-612, 2021.
42. Gao BH, Wu H, Wang X, Ji LL and Chen C: MiR-30c-5p inhibits high glucose-induced EMT and renal fibrogenesis by down-regulation of JAK1 in diabetic nephropathy. Eur Rev Med Pharmacol Sci 24: 1338-1349, 2020.
43. Wang L, Chen X, Wang Y, Zhao L, Zhao X and Wang Y: MiR-30c-5p mediates the effects of panax notoginseng saponins in myocardial ischemia reperfusion injury by inhibiting oxidative stress-induced cell damage. Biomed Pharmacother 125: 109963, 2020.
44. Huntzinger E and Izaurralde E: Gene silencing by microRNAs: Contributions of translational repression and mRNA decay. Nat Rev Genet 12: 99-110, 2011.
45. Martins-Marques T, Ribeiro-Rodrigues T, Batista-Almeida D, Aasen T, Kwak BR and Girao H: Biological functions of connexin43 beyond intercellular communication. Trends Cell Biol 29: 835-847, 2019.
46. Li C, Tian M, Gou Q, Jia YR and Su X: Connexin43 modulates X-ray-induced pyroptosis in human umbilical vein endothelial cells. Biomed Environ Sci 32: 177-188, 2019.
47. Ji H, Qiu R, Gao X, Zhang R, Li X, Hei Z and Yuan D: Propofol attenuates monocyte-endothelial adhesion via modulating connexin43 expression in monocytes. Life Sci 232: 116624, 2019.
48. Meghwani H and Berk BC: MST1 kinase-Cx43-YAP/TAZ pathway mediates disturbed flow endothelial dysfunction. Circ Res 131: 765-767, 2022.
49. Morel S, Chanson M, Nguyen TD, Glass AM, Sarieddine MZ, Meens MJ, Burnier L, Kwak BR and Taffet SM: Titration of the gap junction protein Connexin43 reduces atherogenesis. Thromb Haemost 112: 390-401, 2014.
50. Yin X, Feng L, Ma D, Yin P, Wang X, Hou S, Hao Y, Zhang J, Xin M and Feng J: Roles of astrocytic connexin-43, hemichannels, and gap junctions in oxygen-glucose deprivation/reperfusion injury induced neuroinflammation and the possible regulatory mechanisms of salvianolic acid B and carbenoxolone. J Neuroinflammation 15: 97, 2018.
51. Zhu Y, Chen X, Lu Y, Fan S, Yang Y, Chen Q, Huang Q, Xia L, Wei Y, Zheng J and Liu X: Diphenyleneiodonium enhances P2X7 dependent non-opsonized phagocytosis and suppresses inflammasome activation via blocking CX43-mediated ATP leakage. Pharmacol Res 166: 105470, 2021.
52. Huang Y, Mao Z, Zhang Z, Obata F, Yang X, Zhang X, Huang Y, Mitsui T, Fan J, Takeda M and Yao J: Connexin43 contributes to inflammasome activation and lipopolysaccharide-initiated acute renal injury via modulation of intracellular oxidative status. Antioxid Redox Signal 31: 1194-1212, 2019.
53. Tonkin RS, Bowles C, Perera CJ, Keating BA, Makker PGS, Duffy SS, Lees JG, Tran C, Don AS, Fath T, *et al*: Attenuation of mechanical pain hypersensitivity by treatment with Peptide5, a connexin-43 mimetic peptide, involves inhibition of NLRP3 inflammasome in nerve-injured mice. Exp Neurol 300: 1-12, 2018.
54. Lyon H, Shome A, Rupenthal ID, Green CR and Mugisho OO: Tonabersat inhibits connexin43 hemichannel opening and inflammasome activation in an in vitro retinal epithelial cell model of diabetic retinopathy. Int J Mol Sci 22: 298, 2020.
55. Price GW, Chadjichristos CE, Kavvadas P, Tang SCW, Yiu WH, Green CR, Potter JA, Siamantouras E, Squires PE and Hills CE: Blocking connexin-43 mediated hemichannel activity protects against early tubular injury in experimental chronic kidney disease. Cell Commun Signal 18: 79, 2020.

56. Zhang K, Chai B, Ji H, Chen L, Ma Y, Zhu L, Xu J, Wu Y, Lan Y, Li H, *et al*: Bioglass promotes wound healing by inhibiting endothelial cell pyroptosis through regulation of the connexin 43/reactive oxygen species (ROS) signaling pathway. Lab Invest 102: 90-101, 2022.
57. Xu H, Wang M, Li Y, Shi M, Wang Z, Cao C, Hong Y, Hu B, Zhu H, Zhao Z, *et al*: Blocking connexin 43 and its promotion of ATP release from renal tubular epithelial cells ameliorates renal fibrosis. Cell Death Dis 13: 511, 2022.
58. Xia J, Tian Y, Shao Z, Li C, Ding M, Qi Y, Xu X, Dai K, Wu C, Yao W and Hao C: MALAT1-miR-30c-5p-CTGF/ATG5 axis regulates silica-induced experimental silicosis by mediating EMT in alveolar epithelial cells. Ecotoxicol Environ Saf 249: 114392, 2023.
59. Jiang T, Cai Z, Ji Z, Zou J, Liang Z, Zhang G, Liang Y, Lin H and Tan M: The lncRNA MALAT1/miR-30/spastin axis regulates hippocampal neurite outgrowth. Front Cell Neurosci 14: 555747, 2020.
60. Yi J, Liu D and Xiao J: LncRNA MALAT1 sponges miR-30 to promote osteoblast differentiation of adipose-derived mesenchymal stem cells by promotion of Runx2 expression. Cell Tissue Res 376: 113-121, 2019.